



Electrochemical characterisation of gold on Pt{*hkl*} for ethanol electrocatalysis

Omar A. Hazzazi^a, Gary A. Attard^{*,b}, Peter B. Wells^b, F.J. Vidal-Iglesias^b, Meritxell Casadesus^b

^a Department of Chemistry, Faculty of Applied Science, Umm Al-Qura University, P.O. Box 2897, Makkah, Saudi Arabia

^b School of Chemistry, Main Building, Cardiff University, P.O. Box 912, Cardiff CF10 3AT, UK

ARTICLE INFO

Article history:

Received 16 July 2008

Received in revised form 16 October 2008

Accepted 24 October 2008

Available online 5 November 2008

Keywords:

Cyclic voltammetry

Gold adsorption

Pt{*hkl*}

Ethanol electrooxidation

ABSTRACT

The cyclic voltammetric (CV) behaviour of gold adsorbed on Pt{*hkl*} electrodes is reported. It is found that stepped surfaces vicinal to Pt{111} exhibit preferential adsorption of gold at step sites. However, for stepped surfaces containing Pt{100} terraces, adsorption of gold at step and terrace site occurs with equal probability, although for Pt{*n*11} electrodes with $n < 7$ (i.e. electrodes containing short Pt{100} terraces), slight preference for step site adsorption is still observed. This behaviour is similar to that reported previously for Bi adsorption on Pt{*hkl*} and is interpreted in terms of slower rates of gold atom surface diffusion across Pt{100} vs. Pt{111} terraces. By comparing the electrochemical response of gold adlayers on Pt{*hkl*} with previously published bulk Au{*hkl*} voltammetry, it is deduced that the gold overlayers on Pt{*hkl*} are pseudomorphic in nature. This finding is in agreement with previous UHV and electrochemical results for gold deposition on platinum. Using such gold modified Pt{*hkl*} electrodes as model surfaces, we also report, for the first time, the electrooxidation of ethanol on Au/Pt{*hkl*} in alkaline aqueous solution. The ethanol oxidation reaction (EOR) is shown to be structure sensitive for submonolayer gold coverages. In fact, a maximum in the rate of EOR at platinum sites adjacent to gold islands is observed between approximately 0.4–0.6 monolayers of gold on Pt{100}, Pt{111} and Pt{110} in 0.1 M NaOH(aq). A second electrooxidation state at more positive potentials for $0 < \theta_{\text{Au}} < 1$ ascribed to EOR at pure gold sites is also observed, at least for Pt{111} and Pt{100}. On Pt{111}, the potential range and activity of EOR in this second process is similar to bulk gold whereas for submonolayer gold films on Pt{100}, the peak is shifted to more negative potentials.

© 2008 Elsevier B.V. All rights reserved.

1. Introduction

The adsorption of adatoms on metal electrodes has been studied extensively since it allows for the optimisation of more selective and/or more active electrocatalysts for use in fuel cells [1–6]. This is particularly important if one wishes to utilise biofuels such as ethanol in future fuel cell applications [7–10]. Ethanol is a notoriously difficult molecule to fully electrooxidise (to carbon dioxide) since most electrocatalysts are rather inefficient at breaking the C–C bond of ethanol and therefore, instead, tend to produce C2 side products such as acetic acid and acetaldehyde [11,12]. Hence, much fundamental work has been undertaken to explore the role of defects, adatoms and various electrode materials in facilitating complete activation of ethanol [11,13–17]. Recently, we have been exploring the feasibility of using Pt{*hkl*} electrodes as templates for the formation of well defined monometallic and bimetallic adlayers [18–21]. It is found that so long as the lattice parameter

difference between the adsorbate and Pt is not too dissimilar, good pseudomorphic analogues of the bulk adsorbate Miller index plane may be reproduced using a combination of ‘forced deposition’ and thermal annealing under well defined conditions [18–21]. In addition, interesting results have been reported previously when adatoms are preferentially deposited at stepped surfaces. In this latter case, it has been reported that some adatoms preferentially deposit on step sites whereas some others preferentially deposit on terraces [2–6]. Platinum has been one of the metals that have received most attention in this regard due to its intrinsic catalytic properties. On platinum, copper [2], tin [3], antimony [4], bismuth [3–6] and tellurium [4,6] have all been reported to decorate step sites, whereas selenium [4,6] and sulphur [6] are reported to decorate terrace sites preferentially. This behaviour has been ascribed to differences in work function between platinum and the adsorbate. Those adsorbates exhibiting a lower work function than platinum tend to populate step sites in preference to terraces [6]. However, we have reported that for bismuth adsorbed on Pt{*hkl*}, this type of behaviour is only observed for Pt{*hkl*} planes vicinal to Pt{111} and that for surfaces containing more open planes, random adsorption is observed [22].

* Corresponding author. Tel.: +44 (0)29 20874023; fax: +44 (0)29 20874030.
E-mail address: attard@cardiff.ac.uk (G.A. Attard).

The promotional effect of various adatoms on platinum electrodes used in the electrooxidation of small organic molecules should also be noted [23–29]. The destabilisation of adsorbed poisons such as CO formed during ethanol electrooxidation for example [13,16] may be facilitated to a large extent via bifunctional [13,16] or ligand [30] mechanisms associated with the presence of the adatom.

In this paper, we report the deposition of gold on Pt{*hkl*} in order to investigate the possibility of producing epitaxial and pseudomorphic gold adlayers. Such adlayers afford a rapid and relatively inexpensive method of screening many structural aspects of electrocatalysis [31–33] and in the present context, we wished to apply these advantages to the investigation of ethanol electrooxidation. Since no studies of this reaction on either bulk Au{*hkl*} or gold modified platinum single crystal electrodes are to be found in the literature. In fact, such measurements should provide an interesting comparison for future studies of the EOR on bulk Au{*hkl*} electrodes. It is well-known that gold electrodes afford a significant electrocatalytic activity towards the electrooxidation of organic molecules [34–41] using alkaline aqueous electrolytes but hardly any activity in sulphuric acid [39]. It is thought that the ability of gold to adsorb stable surface OH [42] under alkaline conditions together with the complete absence of adsorbed CO poisoning species [39] may be responsible for this behaviour. Indeed this behaviour of gold makes an interesting comparator with recent studies of small supported gold heterogeneous catalysis that are reported to be extremely active for CO oxidation at low temperature [43,44]. The growth behaviour of gold on Pt{*hkl*} has been reported in UHV by Somorjai et al. [45,46] and Borg et al. [47]. In both cases, pseudomorphic growth of the gold adlayer was reported although gold deposition on clean, reconstructed Pt{100}–hex surfaces caused an immediate lifting of the clean surface reconstruction with significant disorder arising due to the generation of many small Pt{100} islands sitting proud of the surface [47].

In order to form a pseudomorphic gold adlayer on platinum, a contraction of the gold bulk lattice of about 4% would be required. Behm and coworkers also reported the growth of pseudomorphic gold monolayers on Pt{111} using *in situ* STM and an electrochemical underpotential deposition (UPD) process [48,49]. These workers showed that the Stranski–Krastanov growth mode was operative under their experimental conditions with pseudomorphic growth being observed up to two complete gold monolayers followed by relaxation of the film towards the bulk gold lattice constant and 3D nucleation and growth in the third and subsequent layers. Even for a well ordered Pt{111} substrate, these workers also report an important role for steps in the initial nucleation and growth kinetics of gold. Changes in overlayer lattice parameter have recently been discussed in terms of influencing surface electronic structure and hence electrocatalytic behaviour [50–54]. Hence, contrasts between the electrocatalytic activity of submonolayer and multilayer amounts of gold should yield interesting insights since in the former case, the gold lattice is contracted whereas one would expect a multilayer gold film to relax back towards its bulk value, as indeed is reported in Refs. [45–47].

2. Experimental

Platinum single crystals were oriented, cut and polished from small single crystal beads (2.5 mm diameter) as described previously [55]. Platinum metal used to manufacture the single crystal electrodes was supplied by Goodfellow Metals Ltd. (>99.999% purity). The electrodes were flame-annealed and cooled down in a H₂ atmosphere in the usual way [56]. It has been shown that this treatment leads to the generation of well defined surfaces [57].

Electrochemical experiments were carried out in a conventional three-electrode cell with a large Pt counter-electrode and a palladium wire charged with hydrogen was used as a reference electrode. All electrolytes were prepared using 18.2 MΩ cm Milli-Q water and Suprapur (Aristar) grade H₂SO₄. Oxygen was eliminated from the electrochemical cell by bubbling N₂ for 20 min. For ethanol electrooxidation measurements, a second cell was prepared but using a 0.1 M ethanol (99.99%) + 0.1 M NaOH (p.a. grade) instead of sulphuric acid. All potentials are quoted vs. a Pd/H reference.

Gold surface layers, with coverages ranging from submonolayers to one monolayer (ML) were prepared by forced deposition [18] from a dilute gold solution. The concentration of this aqueous solution was 10⁻⁵–10⁻⁶ M in AuCl₃ (Johnson Matthey 99.99% purity). Once the deposition had taken place, the electrode was transferred to an electrochemical cell where the surface was cycled from 0 to 0.85 V until a stable CV was recorded. This had the effect of electrochemically annealing the gold adlayer and manifested itself as a gradual diminution in Pt hydrogen underpotential deposition (H UPD) sites. The determination of the gold coverage was made from an assumption of a one to one correspondence between Pt sites blocked and the amount of gold adsorbed such that the area under the H UPD region of the clean surface was ascribed to residual, free Pt sites. Hence, the ratio of this residual H UPD area to that of the clean surface H UPD charge corresponded to a fractional coverage of gold in monolayers. The immersion in the gold solution and subsequent reduction in hydrogen (forced deposition [18]) was repeated many times in order to increase gold coverage.

3. Results and discussion

3.1. Gold adsorption on Pt{*hkl*}

Fig. 1a–c shows the effects of gold deposition on the three platinum basal planes, Pt{111}, Pt{100} and Pt{110}, respectively. Continuous deposition of gold gradually attenuates all terrace sites, until no signal from the platinum substrate is recorded in the voltammogram profiles. Voltammograms corresponding to one monolayer of gold appear very similar to those corresponding to the gold basal plane [58] (although after multiple potential cycles, no evidence for surface reconstruction peaks of Au{100} or Au{111} [58] are observed – see later). The presence of Pt atoms within a gold overlayer (surface alloys) is not expected from simple thermodynamic considerations, since Au has a lower surface free energy than Pt [59], and thus should be expected to grow layer by layer. Gold overlayers on platinum have been reported to form 2D islands with 3D growth observed at high gold coverage on polycrystalline [60] and single crystalline samples [47].

Upon addition of gold to Pt{100}, the retention of the clean surface CV profile in the potential range 0.0–0.4 V corresponding to hydrogen underpotential deposition (H UPD) and dissolution and anion adsorption–desorption (though continuously diminishing in intensity) suggests that long range order in the residual Pt{100}–(1 × 1) sites is being maintained. In contrast, the Pt{111} “spike” at 0.43 V is quickly diminished even at low gold coverage. Hence, for Au/Pt{111}, rapid diffusion of gold on the close-packed {111} terrace is deduced causing gold to nucleate as small islands over the entire surface leading to the break up of the two dimensional long-range order of the surface (rapid attenuation of Pt{111} “spike”). Conversely, it may be deduced that for Pt{100}, surface diffusion is sufficiently slow such that large (1 × 1) gold islands form, hence preserving the intensity of the 0.33 V vs. Pd/H Pt{100}–(1 × 1) H UPD peak, related to the presence of large Pt{100} terraces, even at gold coverages close to 1 monolayer. For Pt{110} (Fig. 1c) it is not possible to describe the

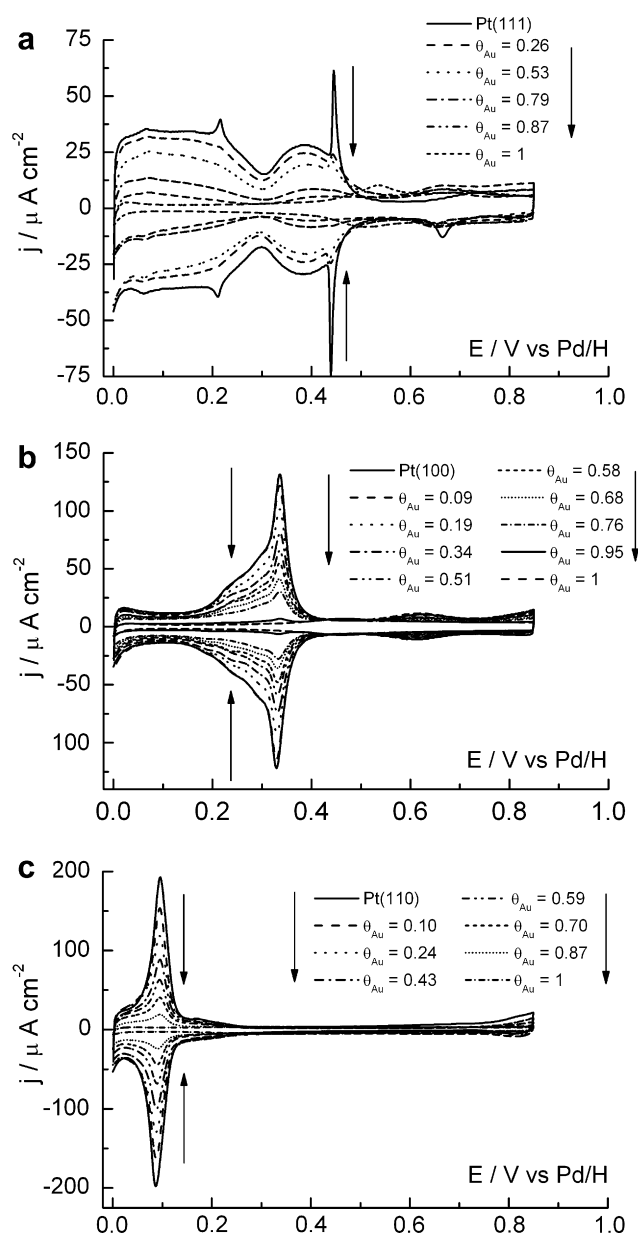


Fig. 1. Voltammograms for consecutive gold depositions onto (a) Pt{111}, (b) Pt{100} and (c) Pt{110}. Test solution: 0.1 M H_2SO_4 . Sweep rate: 50 mV s^{-1} . Arrows indicate change of current density with increasing Au coverage.

microscopic behaviour of Au deposition in such detail from the CV alone since only a gradual blocking of clean surface sites can be observed. In all cases however, it may be asserted that Au should be growing as close-packed islands. Since transition metals deposited on transition metals nearly always exhibit attractive lateral interactions hence generating closely-packed islands [61]. Whether or not it can be determined from this data that the islands are pseudomorphic is another question. However, examination of electrochemical oxide formation behaviour of the films strongly supports this notion.

After full blocking of all Pt H UPD sites by gold adatoms was obtained, the upper potential limit was increased to 1.6 V vs. Pd/H. Fig. 2a–c illustrates the voltammogram response obtained for Pt{111}, Pt{100} and Pt{110} respectively, for the new potential window. No evidence for Pt electrochemical oxide formation was apparent from these data as signified by the complete absence of Pt electrooxidation peaks. For defect free Au{111} surfaces, sharp

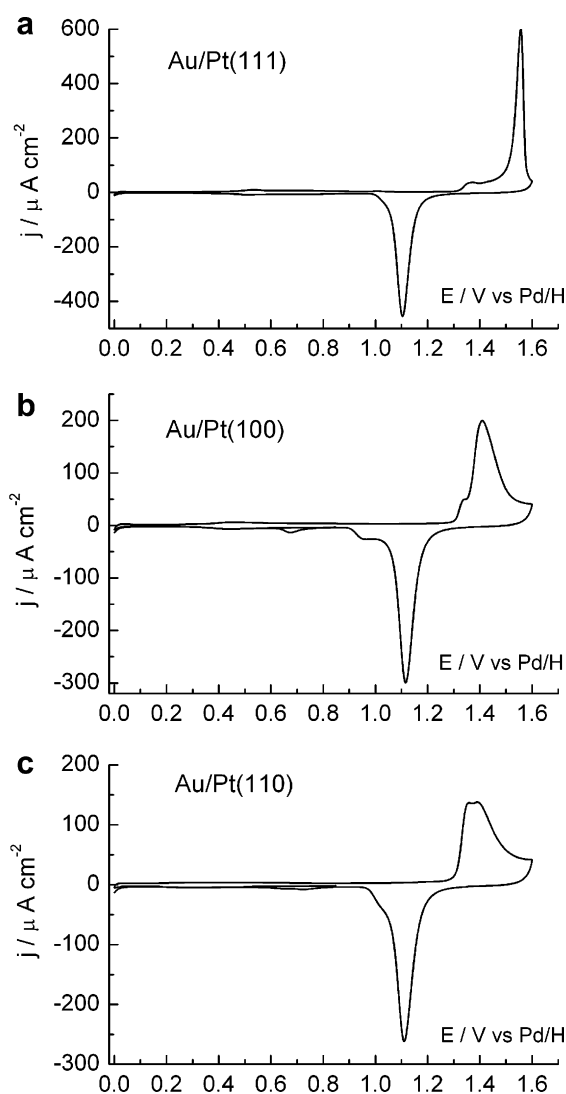


Fig. 2. Oxide potential region (OPR) of gold deposition on Pt flat surfaces in 0.1 M H_2SO_4 at sweep rate 50 mV s^{-1} . (a) 1 ML Au/Pt{111}, (b) 1 ML Au/Pt{100} and (c) 1 ML Au on Pt{110}.

gold electrochemical oxide peaks at 1.5 V (formation) and at 1.1 V (stripping) are reported by Hamelin and Schneeweiss and Kolb [58,62]. Furthermore, these workers also report that a mis-cut of only $\pm 1/2^\circ$ from the Au{111} plane leads to a broadening and a diminution in magnitude of Au{111} electrochemical oxide peaks [63]. For a Au monolayer on Pt{111}, excellent (1×1) pseudomorphic order of the gold adlayer is therefore deduced prior to gold electrochemical oxide formation since such bulk electrochemical gold oxide peaks are reproduced in the gold film supported on Pt{111}. This would also of course agree with previous findings by Behm et al. [48,49].

For both Au/Pt{100} (Fig. 2b) and Au/Pt{110} (Fig. 2c), the shape of the voltammogram in the oxidation region for the Pt electrode fully covered by Au is almost identical to that reported for highly ordered Au single crystals of the same symmetry [58]. Hence, good (1×1) pseudomorphic gold film formation is also deduced for Pt{100} and Pt{110} based on electrochemical analysis. It should be noted that the complete blocking of the H UPD and anion adsorption contributions by gold also coincided with complete blocking of the Pt–O reduction peaks (0.65 V). Hence, the ratio of charges between the Au–O and Pt–O stripping peaks, in addition to the attenuation of H UPD and anion adsorp-

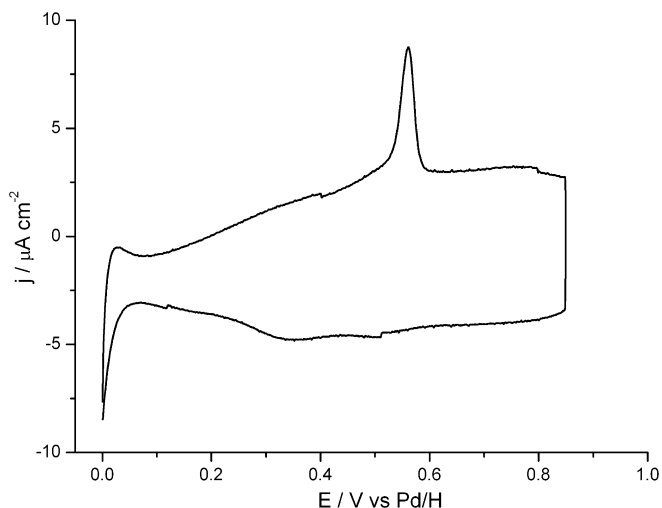


Fig. 3. Ten monolayer equivalents of gold deposited on Pt{100} and subsequently flame-annealed to red heat in a Bunsen flame. First CV obtained after flame-anneal and contact at 0 V (Pd/H) in 0.1 M H₂SO₄ at sweep rate 50 mV s⁻¹. Sharp spike on positive-going potential sweep corresponds to lifting of Au{100}-hex reconstruction [47].

tion desorption, may also be used to determine gold coverages. One final piece of evidence in support of a pseudomorphic growth mode for gold on platinum may be deduced from Fig. 3 which shows the positive-going linear sweep voltammogram of a gold multilayer on Pt{100} but annealed to “cherry red” in a Bunsen flame and cooled in a stream of nitrogen.

It is observed that a large voltammetric peak is observed in the double layer region of the CV. This peak is not observed on subsequent potential excursions and therefore may be identified with the lifting of the Au{100} clean surface reconstruction [48,49].

The possibility of decorating platinum stepped surfaces vicinal to Pt{111} and Pt{100} with gold was also examined in the present study. Since the different adsorption processes, e.g. hydrogen UPD and sulphate/bisulfate adsorption-desorption are sensitive to the site symmetry, it is possible to identify whether the deposition of the adatom is taking place on the Pt terrace or on the Pt step. Stepped surfaces vicinal to Pt{111} were examined first of all.

Fig. 4a, c and e shows the effect of gold adsorption on the voltammetric profile of Pt{755}, Pt{533} and Pt{211}. Initially, there is a diminution in the intensity of the step peak at 0.22 V, without significant change in the anion adsorption-desorption peak at 0.45 V associated with Pt{111} terrace sites. This means that gold adatoms must bind preferentially at the {111} × {100} step sites. Nevertheless, some adsorption of gold adatoms on Pt{111} terraces is seen to commence before *all* step sites are fully blocked. This behaviour of gold is different to bismuth whereby complete blocking of step sites is followed subsequently by adsorption at terrace sites [4–6]. Eventually, all terrace sites are also blocked by gold.

The decoration of steps by gold adatoms in the first stages of the deposition can be explained by the process of surface diffusion combined with the electrostatic attraction of the adatom for the step site [6]. When a gold adatom is deposited at the surface, it diffuses until it reaches a position of minimum energy. When gold adatoms are deposited on the {111} terraces, they move over the surface until they reach a step site, where they are trapped. Since an adatom has a lower potential energy on these sites compared with terrace sites, it remains at the step. Gold adatoms appear to diffuse quickly over the surface during the first stages of deposition. Other adatoms show similar behaviour, such as bismuth [3–6], tellurium [4,6], copper [2], tin [3], antimony [4]. Nevertheless, as mentioned earlier, the selectivity of gold to adsorb at step sites is reduced as compared to bismuth. Consideration of the difference

in work function between gold and platinum and bismuth and platinum would, according to Feliu et al. [6], lead to less of an electrostatic association with the step site dipole moment since the polarity of the Au–Pt bond is much less than that of Bi–Pt [64]. This probably accounts for the slight differences in behaviour between the two adsorbates. Fig. 4b, d and f shows the corresponding electrochemical oxide region for Pt{hkl} surfaces fully blocked with gold. A striking difference between these stepped, vicinal surfaces and Au/Pt{111} is the marked attenuation in the “Au{111}” electrooxidation peak at 1.5 V as a function of step density. Hence, this direct correspondence between step density and electrochemical oxide peak intensity must indicate that the gold films on stepped Pt{111} surfaces are also pseudomorphic. Further close inspection of the CVs reveals that two new gold oxide adsorption peaks at 1.35 V and 1.45 V grow in intensity as surface step density increases. Since the 1.45 V peak is also observed with Au/Pt{100}, we tentatively ascribe the 1.35 V peak to oxide formation on {111} × {100} steps. The increase in step density is also manifested as an increase in the magnitude of the oxide stripping peak at approximately 0.95 V. In order to test these assertions still further (pseudomorphic gold epitaxy coupled with structure sensitivity of gold oxide), stepped ({111} × {100}) surfaces vicinal to Pt{100} were studied using Pt{711}, Pt{11,1,1} and Pt{13,1,1} corresponding to 4, 6 and 7 atom wide terraces respectively.

Fig. 5a, c and e shows the effects of consecutive gold deposits on these Pt single crystals. From the CVs, it is clear that deposition of gold adatoms occurs at the same rate at steps and terraces for both medium and high dosages of gold. Nevertheless, it is observed that the wider the terrace, the more Au is deposited equally on terraces and steps, probably due to the more hindered diffusion to step sites across larger, more open Pt{100} terraces. Thus, for short {100} terraces with {111} × {100} steps, the diffusion of gold from terrace to step site is achieved more readily (see initial deposit on Pt{711}). After the initial gold deposit, subsequent behaviour is governed by little apparent preference of gold atoms for either step or terrace sites.

Inspection of the gold oxide peaks formed at highest gold coverages (complete blocking of platinum sites) indicates systematic changes in the structure of the peaks as a function of step density and terrace type. Since these peaks are also consistent with bulk gold single crystalline behaviour [65], one may deduce that gold overlayers are pseudomorphic with the platinum substrate. Furthermore, the growth in the intensity of the 1.45 V oxide peak as a function of increasing Pt{100} terrace width also confirms that, as for surfaces vicinal to Pt{111}, this peak may be ascribed to gold oxide formation at {100} sites. The corresponding decrease in the 1.35 V “step {111}” peak as a function of decreasing step density also confirms the nature of oxide formation in this case, namely adsorption at {111} step sites. Hence, it may be possible to study stepped gold single crystal surfaces using platinum single crystals as a “template” whilst avoiding problems associated with the facile reconstruction that is observed with pure gold surfaces [58,65].

3.2. Ethanol electrooxidation on Au/Pt{hkl} surfaces

Fig. 6 shows the initial, positive-going potential sweep obtained for ethanol electrooxidation in alkaline electrolyte for the three basal planes of platinum as a function of fractional gold coverage.

The peak between 0.6 V and 0.8 V (peak A) is ascribed to electrooxidation on platinum sites since this overlaps with the potential range found with clean platinum. All three gold-modified planes exhibited a marked maximum in electrocatalytic activity at approximately $\theta_{Au} = 0.4$ –0.6 for peak A. This suggests strongly that platinum sites adjacent to gold islands are more active than gold-free sites and that the maximum in electrocatalytic rate is related to the surface density of such sites. As all platinum sites are

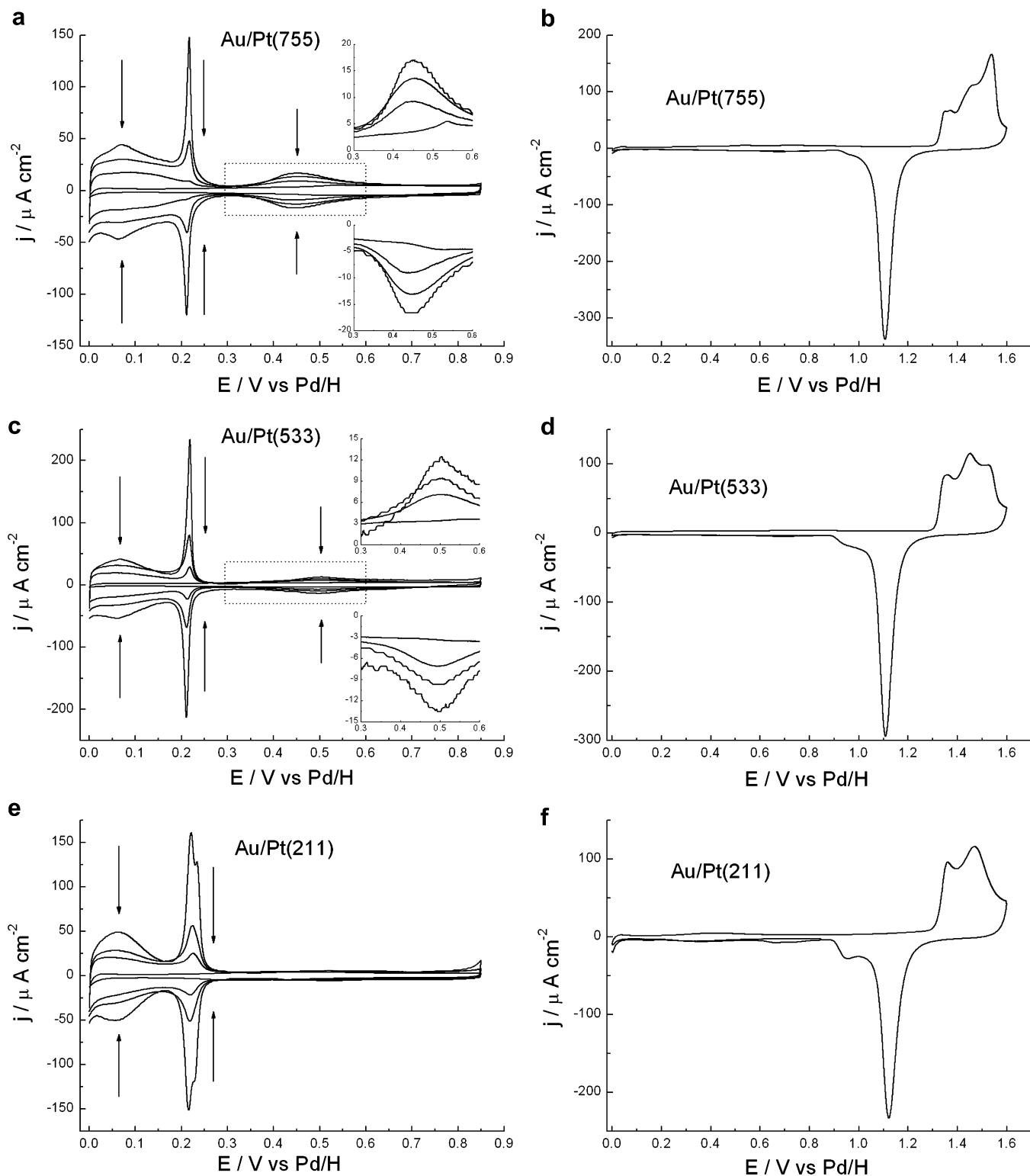


Fig. 4. CVs of gold deposition on Pt stepped surfaces vicinal to {111} terraces in 0.1 M H_2SO_4 at sweep rate 50 mV s^{-1} . Arrows indicate changes of current density with increasing Au coverage: (a), (b) Au/Pt(755); (c), (d) Au/Pt(533); (e), (f) Au/Pt(211), (b), (d) and (f) represent the oxide potential region for the corresponding Pt{*hkl*} surface fully blocked with gold.

eventually blocked by gold, the electrooxidation current in peak A falls with only a weak residual peak due to some free Pt sites remaining. In terms of overall catalytic activity, only taking into account current densities at the peak maxima in the cyclic voltammograms from Fig. 6, Pt{111} > Pt{110} > Pt{100} and interestingly, this order also holds for gold films on Pt{*hkl*} for

$\theta_{\text{Au}} \approx 0.5$ (Fig. 7). Hence, the EOR reaction is structure sensitive with Au/Pt{111} surfaces in general exhibiting the greatest electrooxidation currents. Whether complete oxidation of ethanol to carbon dioxide or partial oxidation to ethanoic acid and other organic intermediates is taking place is unknown at the present time. Unfortunately, preliminary DEMS measurements proved unreliable

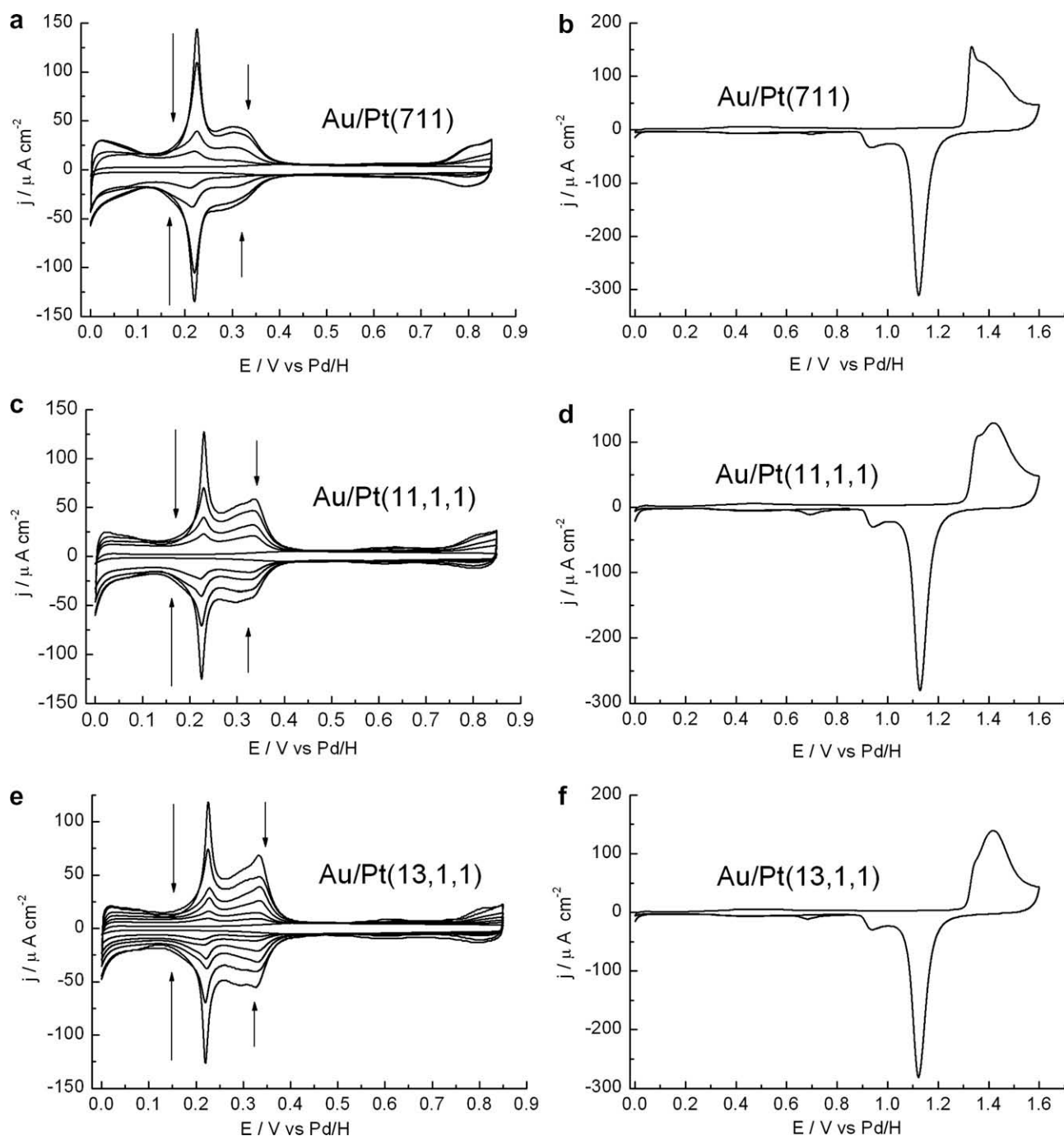


Fig. 5. CVs of gold deposition on Pt stepped surfaces vicinal to {100} terraces in 0.1 M H_2SO_4 at sweep rate 50 mV s^{-1} . Arrows indicate changes of current density with increasing Au coverage: (a), (b) Au/Pt(711); (c), (d) Au/Pt(11,1,1); (e), (f) Au/Pt(13,1,1), (b), (d) and (f) represent the oxide potential region for the corresponding Pt{hkl} surface fully blocked with gold.

due to reaction between the alkaline aqueous electrolyte and evolved carbon dioxide [66].

For Au on Pt{111} and Pt{100} (although not for Pt{110}), a second EOR peak is observed at potentials positive of 1.0 V for $0 < \theta_{\text{Au}} < 1$ which is ascribed to ethanol electrooxidation on pure gold sites since this potential range overlaps with the EOR peak seen using a bulk Au{643} electrode. Inspection of peak B behaviour confirms that it grows in intensity as a function of fractional gold coverage up to $\theta_{\text{Au}} = 1$ and then saturates. On Pt{111}, the magnitude of peak B reaches an intensity close to that exhibited by Au{643} at highest gold coverages (Fig. 7). Hence, the following trends for peak B may be deduced:

- For gold on Pt{111}, a well-developed peak B is observed at the same potential and of similar magnitude as found using bulk Au{643}. Therefore, it is deduced that gold films on Pt{111} readily adopt an electronic structure giving rise to similar electrocatalytic behaviour as bulk gold, even at submonolayer coverages.
- For gold on Pt{100}, peak B is situated at slightly more negative potentials than observed for Au{643} for $0 < \theta_{\text{Au}} < 1$. However, for coverages of gold > 1 monolayer, a shoulder peak at potentials similar to Au{643} is observed (not shown). Therefore, in contrast to the behaviour reported for Au on Pt{111}, it appears that monoatomic thick gold films are electronically distinguishable

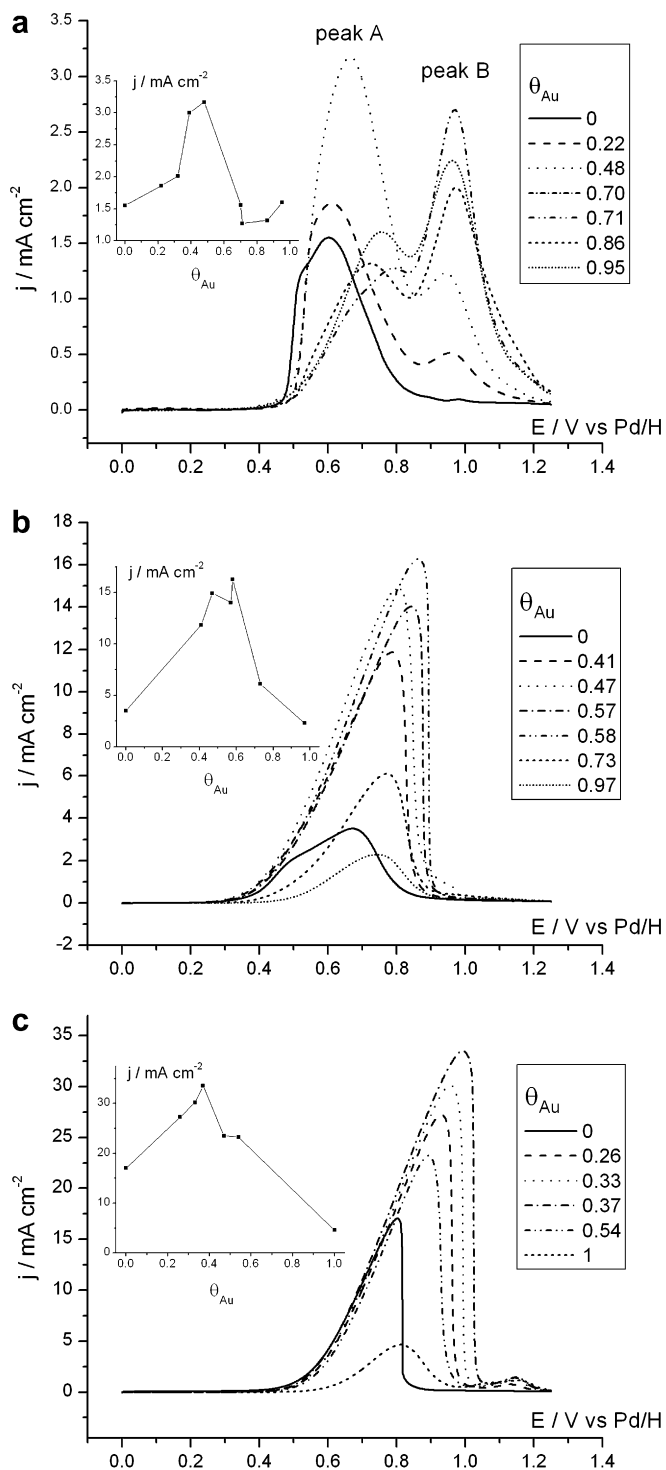


Fig. 6. The initial, positive-going potential sweep obtained for ethanol electrooxidation in alkaline electrolyte for the three basal planes of platinum as a function of fractional gold coverage. Electrolyte: 0.1 M ethanol in 0.1 M NaOH (aq). Sweep rate 50 mV s^{-1} . (a) Pt{100}, (b) Pt{110} and (c) Pt{111}. Insets indicate changes in ethanol electrooxidation current density for peak A (see text) as a function of gold coverage.

from bulk gold, at least in relation to EOR activity but for thicker films, bulk gold behaviour obtains. Since in the earlier part of the paper it was established that the gold film was pseudomorphic with the Pt{100} substrate, this must reflect perturbation by the Pt on the gold film giving rise to a more “Pt-like” behaviour

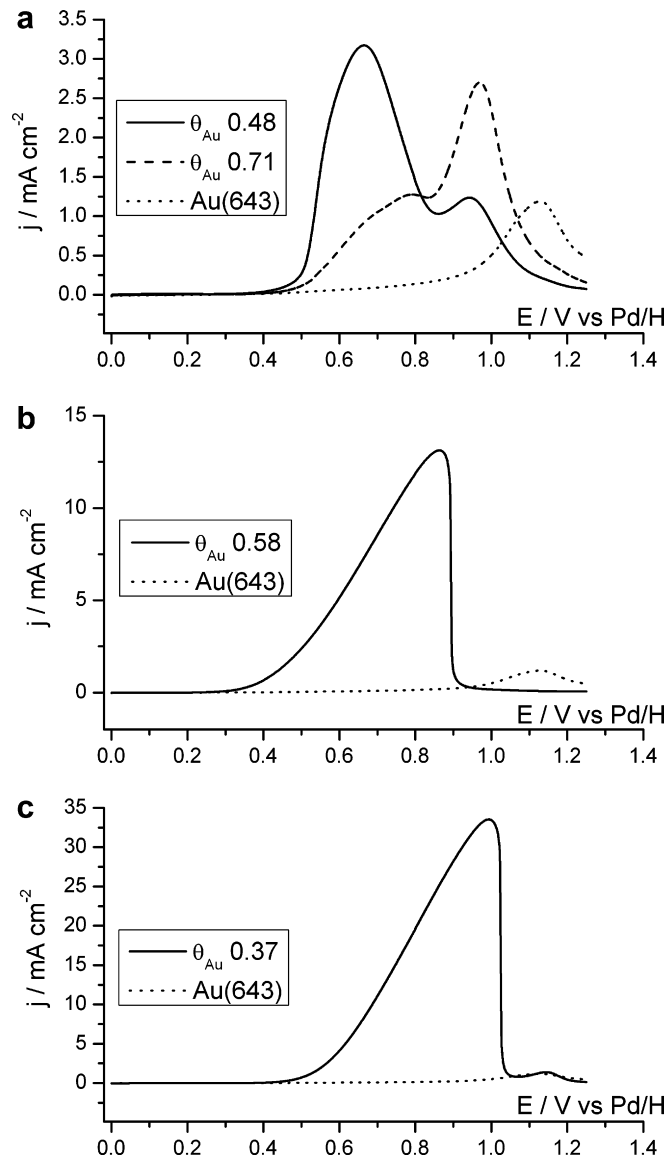


Fig. 7. Comparison of ethanol electrooxidation behaviour in aqueous alkaline electrolyte at optimal submonolayer gold coverage on (a) Pt{100}, (b) Pt{110} and (c) Pt{111} with that on Au{643}. Electrolyte: 0.1 M ethanol in 0.1 M NaOH (aq). Sweep rate 50 mV s^{-1} .

and a correspondingly lower overpotential for EOR relative to pure gold.

- For Au/Pt{110}, no evidence for the presence of “peak B” could be seen for $0 < \theta_{\text{Au}} < 1$. For coverages of gold > 1 monolayer, a broad, low intensity peak could occasionally be observed at potentials $> 1 \text{ V}$ which we ascribe to EOR activity on two or more monoatomic thick gold islands. Hence, the absence of peak B for gold on Pt{110} must reflect a strongly perturbed electronic structure in the monolayer film as compared to bulk gold (as described for Au/Pt{100}).

4. Conclusion

By comparing the electrochemical response of gold adlayers on Pt{hkl} with previously published bulk Au{hkl} voltammetry [58,65], it is deduced that the gold overlayers on Pt{hkl} are pseudomorphic in nature. This finding is in agreement with previous UHV and electrochemical results [45–47] for gold deposition on

Pt{111}. For gold adsorbed on Pt{hkl} electrodes, it is found that stepped surfaces vicinal to Pt{111} exhibit preferential adsorption of gold at step sites. However, for stepped surfaces containing Pt{100} terraces, adsorption of gold at step and terrace site occurs with equal probability, although for narrow Pt{100} terraces, some preference for step site adsorption is still maintained. This behaviour is similar to that reported previously by ourselves for Bi adsorption on Pt{hkl} [67] and is interpreted in terms of slower rates of gold atom surface diffusion across Pt{100} vs. Pt{111} terraces. Using such gold modified Pt{hkl} electrodes as model surfaces, we also investigated the electrooxidation of ethanol on Au/Pt{hkl} in alkaline aqueous media. Larger electrooxidation currents are observed at pH = 13 for submonolayer gold coverages relative to clean platinum. In fact, a maximum in the rate of EOR at platinum sites adjacent to gold islands is observed between approximately 0.5 and 0.6 monolayers of gold on Pt{100}, Pt{111} and Pt{110} in 0.1 M NaOH(aq). The ethanol oxidation reaction (EOR) was shown to be structure sensitive with {111} > {110} > {100} in terms of ethanol oxidation reaction rate based on current density at EOR peak maxima. A second electrooxidation state at more positive potentials for $0 < \theta_{Au} < 1$ ascribed to EOR at pure gold sites is also observed, at least for Pt{111} and Pt{100}. The potential range and activity of EOR in this second process on Pt{111} was similar to bulk gold whereas for Pt{100}, the peak is shifted to more negative potentials whilst for Pt{110} the peak is not observed at all. This behaviour is speculated to be a reflection of electronic properties within the gold film deviating from bulk gold in the order $Au\{643\} \approx Au/Pt\{111\}$ ($0 < \theta_{Au} < 1$), $Au\{643\} \approx Au/Pt\{100\}$ ($\theta_{Au} > 1$) and $Au/Pt\{110\}$ only approaching the electrocatalytic activity of bulk Au{643} at coverages well in excess of one monolayer.

Acknowledgement

The authors would like to thank the EPSRC for financial support. Omar A. Hazzazi expresses his thanks to Saudi Arabian Government for financial support.

References

- [1] C.K. Rhee, M. Wakisaka, Y.V. Tolmachev, C.M. Johnston, R. Haasch, K. Attenkofer, G.Q. Lu, H. You, A. Wieckowski, J. Electroanal. Chem. 554–555 (2003) 367.
- [2] L.J. Buller, E. Herrero, R. Gómez, J.M. Feliu, H.D. Abruña, J. Chem. Soc. Faraday Trans. 92 (1996) 3757.
- [3] H. Massong, S. Tillmann, T. Langkau, E.A. Abd El Meguid, H. Baltruschat, Electrochim. Acta 44 (1998) 1379.
- [4] M.D. Maciá, E. Herrero, J.M. Feliu, Electrochim. Acta 47 (2002) 3653.
- [5] J. Clavilier, J.M. Feliu, A. Aldaz, J. Electroanal. Chem. 243 (1988) 419.
- [6] E. Herrero, V. Climent, J.M. Feliu, Electrochem. Commun. 2 (2000) 636.
- [7] F. Vigier, C. Coutanceau, A. Perrard, E.M. Belgsir, C. Lamy, J. Appl. Electrochem. 34 (2004) 439.
- [8] C. Lamy, S. Rousseau, E.M. Belgsir, C. Coutanceau, J.M. Léger, Electrochim. Acta 49 (2004) 3901.
- [9] C. Lamy, A. Lima, V. LeRhun, F. Delime, C. Coutanceau, J.M. Léger, J. Power Sources 105 (2002) 283.
- [10] J. Wang, S. Wasmus, R.F. Savinell, J. Electrochem. Soc. 142 (1995) 4218.
- [11] H. Wang, Z. Jusys, R.J. Behm, J. Power Sources 154 (2006) 351.
- [12] H. Wang, Z. Jusys, R. J. Behm, J. Phys. Chem. B 108 (2004) 19413.
- [13] N. Fujiwara, K.A. Friedrich, U. Stimming, J. Electroanal. Chem. 472 (1999) 120.
- [14] D.J. Tarnowski, C. Korzeniewski, J. Phys. Chem. B 101 (1997) 253.
- [15] L. Jiang, L. Colmenares, Z. Jusys, G.Q. Sun, R.J. Behm, Electrochim. Acta 53 (2007) 377.
- [16] V. Del Colle, A. Berná, G. Tremiliosi-Filho, E. Herrero, J.M. Feliu, Phys. Chem. Chem. Phys. 10 (2008) 3766.
- [17] E. Antolini, J. Power Sources 170 (2007) 1.
- [18] F.J. Vidal-Iglesias, A. Al-Akl, D.J. Watson, G.A. Attard, Electrochem. Commun. 8 (2006) 1147.
- [19] F.J. Vidal-Iglesias, A. Al-Akl, D. Watson, G.A. Attard, J. Electroanal. Chem. 611 (2007) 117.
- [20] S.E. Huxter, G.A. Attard, Electrochem. Commun. 8 (2006) 1806.
- [21] L. Fang, F.J. Vidal-Iglesias, S.E. Huxter, G.A. Attard, J. Electroanal. Chem. 622 (2008) 73.
- [22] G.A. Attard, A. Ahmadi, D. Jenkins, O.A. Hazzazi, P.B. Wells, K.G. Griffin, P. Johnston, J.E. Gillies, Chem. Phys. Chem. 4 (2) (2003) 123.
- [23] S.P.E. Smith, K.F. Ben-Dor, H.D. Abruña, Langmuir 16 (2000) 787.
- [24] S.P.E. Smith, K.F. Ben-Dor, H.D. Abruña, Langmuir 15 (1999) 7325.
- [25] M.D. Maciá, E. Herrero, J.M. Feliu, A. Aldaz, Electrochem. Commun. 1 (1999) 87.
- [26] E. Herrero, A. Fernández-Vega, J.M. Feliu, A. Aldaz, J. Electroanal. Chem. 350 (1993) 73.
- [27] S.A. Campbell, R. Parsons, J. Chem. Soc. Faraday Trans. 88 (1992) 833.
- [28] M.D. Maciá, E. Herrero, J.M. Feliu, J. Electroanal. Chem. 554–555 (2003) 25.
- [29] W. Vielstich, A. Lamm, H.A. Gasteiger (Eds.), Handbook of Fuel Cells, Wiley, 2003.
- [30] T. Frelink, W. Visscher, J.A.R. van Veen, Surf. Sci. 335 (1995) 353.
- [31] V. Climent, N.M. Markovic, P.N. Ross, J. Phys. Chem. B 104 (2000) 3116.
- [32] M. Baldauf, D.M. Kolb, J. Phys. Chem. 100 (1996) 11375.
- [33] R. Gómez, A. Rodes, J.M. Pérez, J.M. Feliu, A. Aldaz, Surf. Sci. 344 (1995) 85.
- [34] R.R. Adzic, M.W. Hsiao, E.B. Yeager, J. Electroanal. Chem. 260 (1989) 475.
- [35] M. Tominaga, T. Shimazoe, M. Nagashima, H. Kusuda, A. Kubo, Y. Kuwahara, I. Taniguchi, J. Electroanal. Chem. 570 (2006) 37.
- [36] M.E. Gallagher, B.B. Blizanac, C.A. Lucas, P.N. Ross, N.M. Marković, Surf. Sci. 582 (2005) 215.
- [37] Z. Borkowska, A. Tymosiak-Zielinska, G. Shul, Electrochim. Acta 49 (2004) 1209.
- [38] D. Geng, G. Lu, J. Nanopart. Res. 9 (2007) 1145.
- [39] G. Tremiliosi-Filho, E.R. Gonzalez, A.J. Motheo, E.M. Belgsir, J.-M. Léger, C. Lamy, J. Electroanal. Chem. 444 (1998) 31.
- [40] R.R. Adzic, M. Avramov-Ivic, J. Catal. 101 (1986) 532.
- [41] T. Łuczak, J. Appl. Electrochem. 37 (2007) 461.
- [42] N. Tateishi, K. Nishimura, K. Yahikozawa, M. Nakagawa, M. Yamada, Y. Takasu, J. Electroanal. Chem. 352 (1993) 243.
- [43] M. Haruta, M. Daté, Appl. Catal. A-Gen. 222 (2001) 427.
- [44] M. Haruta, S. Tsubota, T. Kobayashi, H. Kageyama, M.J. Genet, B. Delmon, J. Catal. 144 (1993) 175.
- [45] J.W.A. Sachtler, M.A. van Hove, J.P. Bibérian, G.A. Somorjai, Surf. Sci. 110 (1981) 19.
- [46] J.W.A. Sachtler, M.A. van Hove, J.P. Bibérian, G.A. Somorjai, Phys. Rev. Lett. 45 (1980) 1601.
- [47] C. Berg, H.J. Venvik, F. Strisland, A. Ramstad, A. Borg, Surf. Sci. 409 (1998) 1.
- [48] E. Sibert, F. Ozanam, F. Maroun, R.J. Behm, O.M. Magnussen, Surf. Sci. 572 (2004) 115.
- [49] E. Sibert, F. Ozanam, F. Maroun, O.M. Magnussen, R.J. Behm, Phys. Rev. Lett. 90 (2003) 056102/1.
- [50] C. Xu, D.W. Goodman, J. Phys. Chem. 100 (1996) 245.
- [51] M. Mavrikakis, B. Hammer, J.K. Nørskov, Phys. Rev. Lett. 81 (1998) 2819.
- [52] M.Ø. Pedersen, S. Helveg, A. Ruban, I. Stensgaard, E. Lægsgaard, J.K. Nørskov, F. Besenbacher, Surf. Sci. 426 (1999) 395.
- [53] A. Logadottir, J.K. Nørskov, Surf. Sci. 489 (2001) 135.
- [54] L.A. Kibler, A.M. El-Aziz, D.M. Kolb, J. Mol. Catal. A-Chem. 199 (2003) 57.
- [55] J. Clavilier, D. Armand, S.G. Sun, M. Petit, J. Electroanal. Chem. 205 (1986) 267.
- [56] A. Rodes, M.A. Zamakhchari, K. El Achi, J. Clavilier, J. Electroanal. Chem. 305 (1991) 115.
- [57] A. Al-Akl, G. Attard, R. Price, B. Timothy, Phys. Chem. Chem. Phys. 3 (2001) 3261.
- [58] A. Hamelin, J. Electroanal. Chem. 407 (1996) 1.
- [59] L.Z. Mezey, J. Gibber, Jpn. J. Appl. Phys. 21 (1982) 19.
- [60] M.N. Desic, M.M. Popovic, M.D. Obradovic, L.M. Vracar, B.N. Grgur, J. Serb. Chem. Soc. 70 (2005) 231.
- [61] E. Bauer, in: D.A. King, D.P. Woodruff (Eds.), Chemical Physics of Solid Surfaces and Heterogeneous Catalysis, Vol. 111a, Elsevier, Amsterdam, 1982.
- [62] M. Schneeweiss, D. Kolb, Solid State Ion. 94 (1997) 171.
- [63] M.A. Schneeweiss, D.M. Kolb, D. Liu, D. Mandler, Can. J. Chem. 75 (11) (1997) 1703.
- [64] M.T. Paffett, C.T. Campbell, T.N. Taylor, J. Chem. Phys. 85 (10) (1986) 6176.
- [65] A. Hamelin, J. Electroanal. Chem. 407 (1996) 13.
- [66] H. Baltruschat, Private Communication.
- [67] D.J. Jenkins, A.M.S. Alabdulrahman, G.A. Attard, K.G. Griffin, P. Johnston, P.B. Wells, J. Catal. 234 (2005) 230.